Towards the automatic detection of critical thinking through EEG and facial emotion recognition.

Hugo G. Gonzalez-Hernandez
Tecnologico de Monterrey
Escuela de Ingeniería y Ciencias
Av. Eugenio Garza Sada 2501
Monterrey 64849, NL, México
ORCID: 0000-0001-6495-9980

Dafne V. Peña-Cortés
Tecnologico de Monterrey
Escuela de Ingeniería y Ciencias
Av. Eugenio Garza Sada 2501
Monterrey 64849, NL, México
ORCID: 0000-0001-5451-729X

A. Flores-Amado
Tecnologico de Monterrey
Escuela de Ingeniería y Ciencias
Av. Eugenio Garza Sada 2501
Monterrey 64849, NL, México
afloresam@tec.mx

Alberto Oliart-Ros
Tecnologico de Monterrey
Escuela de Ingeniería y Ciencias
Av. Eugenio Garza Sada 2501
Monterrey 64849, NL, México
aoliart@tec.mx

Miguel A. Martinez-Ayala
Tecnologico de Monterrey
Escuela de Ingeniería y Ciencias
Av. Eugenio Garza Sada 2501
Monterrey 64849, NL, México
a01734990@tec.mx

Roberto J. Mora-Salinas
Tecnologico de Monterrey
Escuela de Ingeniería y Ciencias
Av. Eugenio Garza Sada 2501
Monterrey 64849, NL, México
rjmora@tec.mx

***Abstract*—The main goal of this research is to propose a quantitative approach to identify critical thinking in undergraduate engineering students by leveraging electroencephalogram (EEG) measurements, facial emotion recognition and machine learning techniques. Measurements were taken by recording the face of the subjects and acquiring EEG signals from a wearable device. We explore the use of chaotic descriptors such as Lyapunov exponents, fractal dimension, Hurst exponent and approximate entropy to extract meaningful information from EEG signals. Subsequently we tested different machine learning algorithms to classify EEG signals and analyze the onset of critical thinking. An experiment was conducted in which students engaged in problem-based learning scenarios while wearing portable EEG devices. The collected data were then analyzed to discern patterns and discriminate between relevant, irrelevant, and false information in EEG signals. The experimental setup involved measuring the EEG signals from engineering students as they solved problem-based learning scenarios. The results demonstrated the ability to distinguish between different sections of a video based on brain activity, with false, relevant, and irrelevant information. Some findings include the left frontal electrode with the theta frequency band exhibiting the highest distinguishability for relevant information. From the experiments, we identified the Hurst exponent and approximated entropy as the most relevant descriptors for classification. The main contribution of this study is to offer an approach to decode critical thinking in engineering undergraduate students using EEG measurements and machine learning techniques.**

***Index Terms*—Facial Emotion Recognition, Electroencephalogram, Higher Education, Educational Innovation, Critical Thinking, Chaotic Descriptors, Machine Learning.**

I. Introduction

Critical Thinking (CT) is an essential skill to develop in engineering students, several works have been reported on this topic from different perspectives [1], but only few scholars tackle the problem of assessing critical thinking. To evaluate the progress of a student in developing (CT) skills, a detection method should be revised. Some approaches have been reported using electroencephalogram (EEG) signals [2]. We take advantage of this approach and introduce a facial emotion recognition to reinforce such detection. The aim of this work is to link the process of critical thinking to EEG and facial expression recognition in engineering students solving a Problem-Based Learning assessment. Recordings of the face of the subjects and EEG signals acquired from a wearable device are proposed as an indicator to measure critical thinking. EEG signals were filtered and processed using chaos theory, while face recordings were decomposed in individual frames, and both groups of data were used for classification.

Facial recognition is often used in video clips of subjects to classify between human emotions, just like happiness, anger, sadness, surprise, among others. Some already studied geometric techniques to extract features and identify emotions include the location of key facial points and converting them in a vector using euclidean distance [3], construction of matrices with the facial points and getting a vector from their convolution [4], work with databases for geometric features and applying k-means to cluster most different frames [5], and simply getting the distance between facial postures in a neutral state and when smiling [6].

There is also research about machine learning methods for emotion classification, specifically neural networks. Some examples include a study where the variation of gray values of pixels within the eye is taken as input for an autoassociative neural network model [7], the use of multiple pre-trained convolutional neural networks [5], even the calculation of an emotion index of music video clips according to the expressions of the artist determined by SIFT algorithm and neural networks [8]. Models correcting and perfecting themselves are very interesting and there is a few studies about it, mentioning methods like a two-stage convolution network for continuous dimensional emotion recognition, where the first stage generates a first result that is fed to the second for correction, this kind of network can learn and adapt to different attention levels and focuses [9]. Another interesting work in this line proposes a stationary wavelet transform that extracts facial expression features in spectral and spatial domains, it obtains information of muscle movements for most facial expressions, then it goes into a neural network trained with a back propagation algorithm [10].

SVM models are also effective according to different studies, involving real-time detection of emotions using an SVM classifier with increased efficiency [11] and the procurance of a fixed length feature vector for all sample images and the introduction of them to k-nearest neighbours and SVMs with several kinds of function kernels [12].

Multiple reviews where inspected to find the most appropriate and efficient method to extract information about features or complete facial expressions, a few of them include a comparative study with methodologies based on accuracy, tools, advantages and disadvantages [13], a survey on methods for detection from image, feature extraction and classification [14] and a thoroughly review of sensors, machine learning methods and techniques for emotion recognition in recent years [15].

It is important to mention that machine learning or deep learning can be applied not only with face points or features as input but some studies also consider eye gaze direction and head pose as inputs to the model. Examples include the study by Samadiani and colleagues, who focused on happy emotion considering severe head pose variations using a neural network with long-short term memory to extract features [6]. Wu, Du, Li and collaborators also took head pose and eye gaze into account for credibility and as complements to facial expression features [16]. There is another study where head motion and facial appearance features were extracted to recognize spontaneous facial expressions with Bayesian networks and its results show that head motion features matter and improve performance of emotion tagging [17].

Of course, the statistical approach was explored too. There is a innovative study where a representative set of frames was obtained in the eigenspace domain and Principal Component Analysis (PCA) technique was used to capture facial expression dynamics, reducing computational time significantly [18].

In this study, a different approach is proposed in order to discover if facial recognition can be used effectively to identify critical thinking like it has worked before to classify emotions. A previous study shows positive results about using EEG signals processed with chaos theory to discriminate when undergraduate students are presented with relevant, irrelevant and false information. This work repeats the same process to back up the obtained results from classification of facial expression recordings using a convolutional neural network, which is the main focus of this experiment.

Given the intentions of this work, more research was conducted to obtain knowledge about the context of facial recognition in combination with biosignals for classification. In terms of EEG, which is the one intended to use, four studies were found. One shows the use of a multimodal attention network that uses bilinear pooling based on low-rank decomposition to calculate the weights of facial features and EEG features in fusion [19]. The next talks about continuous emotion recognition for deaf subjects, the differential entropy of EEG was obtained, as well as facial landmarks for six facial features, long short-term memory networks were used for level fusion and capturing temporal dynamics of emotions [20]. Other study applied decision level fusion for detection of emotions, specifically power spectrum density features of EEG were extracted [21]. The last paper was aiming to find the emotional charge of videos according to emotions of the audience, long short-term memory recurrent neural networks and Continuous Conditional Random Fields were used for the recognition to take place automatically and continuously [22], it is interesting that results show facial expressions were more helpful than EEG signals.

However, not only EEG was considered for the research. An engaging paper mentions the detection of a player's emotions with heart beat and facial expressions, they employed a bidirectional long short-term memory network for learning HR features and a convolutional neural network to learn the facial features, to fuse both features, the SOM-BP network was employed [23]. Others proposed a new multimodal neural design which takes audio and visual data and combines them to be the input for a hybrid network, spacial and temporal features from video are fused with Mel-Frequency Cepstral Coefficients and a Softmax classifier is used [24]. Lastly, Saganowski and colleagues created a dataset dedicated to test emotion recognition from facial expressions and physiological responses; it was obtained with wearables in parallel with upper-body videos [25].

The rest of this paper is organized as follows. Section II contains in detail the proposed method to detect critical thinking, including the data collection procedure, and the processing of EEG signals and videos. Section III shows some results of applying the proposed method and finally, in Section IV we give some conclusions.

II. Critical thinking detection

In this study, a non-traditional approach is proposed in order to find out if facial recognition can be used effectively to identify critical thinking as it has worked before to classify emotions. A previous study shows positive results about using EEG signals to discriminate when undergraduate students are presented with relevant, irrelevant and false information [2]. This work uses some part of the process therein to back up the obtained results using classification of facial expression recordings using a convolutional neural network, which is the main focus of this experiment.

The proposed experiment aimed to assess critical thinking during an activity designed using the Problem-Based Learning (PBL) methodology. Students were presented with a real or plausible real-life engineering problem. They are tasked with identifying the necessary knowledge, which they may not initially possess, to analyze the problem and devise a strategy to address the questions raised within the scenario.

Students were exposed to a video presenting the problematic situation. The video incorporated moments with false information related to the scenario under examination. Detecting false information or fallacies during the analysis of problematic situations served as an indicator of the occurrence of critical thinking. Another indicator was the ability to distinguish between relevant and irrelevant information within the presented scenario. Table I shows the information contained in each one of the segments of the video.

TABLE I
TIMESTAMPS FOR SECTIONS IN THE VIDEO OF THE DESIGNED PBL.

Time (s)	Type of information
0:02-0:10	Title screen
0:10-1:50	Set of instructions
2:27-2:45	Irrelevant information 1
3:00-3:08	False information 1
3:18-3:48	Relevant information
3:58-4:04	False information 2
4:39-4:50	Irrelevant information 2
5:36-6:03	Triggering questions

Raw data from EEG was used to generate a 4-dimensional vector built with chaotic descriptors, namely Largest Lyapunov Exponent (LLE), Hurst exponent (H), Correlation dimension (Dg), and approximated entropy, further details on this technique can be found in [26]. This vector represents a point in a 4-dimensional space called the descriptor space. Each filtered EEG signal combination (electrode and brainwave) is represented as a point in this space, and its location corresponds to the reaction of the student to false, relevant or irrelevant information. The portable EEG used is a `MUSE 2` device with four electrodes: left frontal (AF3), right frontal (AF4), left temporal (TP7) and right temporal (TP8). Using this the descriptor space, it is possible to identify different reactions to the different information sections.

For the experiment, the students performed the following steps, after signing a consent form:

1) The `MUSE 2` headband was activated and connected to a computer via Bluetooth.
2) Sensors contact were inspected to ensure minimal noise and avoid measurement errors.
3) When the student was ready, the video was started and the data were recorded simultaneously. The students watched the video carefully, and data recording concluded upon video completion. Data collection was started using a custom software, developed in a previous study [26], with an additional feature to record the student's facial expressions.
4) The collected data were subsequently processed and stored in the cloud, specifically within a Google Drive folder for future analysis.

The objective is to know if the 5 delimited sections are differentiable according to brain activity and facial expressions. To achieve that, the obtained EEG signals must be classified, this was made with *MATLAB*'s *Classification Learner* application. All the points corresponding to a single section, a single electrode and a single frequency band (brainwave) were grouped and tested against another of these clusters, mainly to observe if there is a boundary that separates them in descriptor space.

The face recording of each student was divided according to the time limits of each section. After, the videos were converted to images and saved in a folder with the name of the section they belong to, labeling them. The folders are used as the dataset. Finally, the *image dataset from directory* function of the *Tensorflow* library is used to infer the pairs of image and label. The dataset is split into training and validation set, the latter is formed by 25% of the images.

A. Data collection

Carrying out the experiment allowed us to obtain the EEG measurements for each student when they watched a video. As it was mentioned, this is possible thanks to a mobile headset called *MUSE 2* that provides this bio-signal. An open-source application was used to establish a connection with the headset and receive the raw data of the four electrodes associated with both frontal and temporal brain lobes.

As the data is streamed, a custom-made application makes possible the interaction with the user. The application has a very intuitive GUI (Graphical User Interface) where the user can see the streamed data in graphs and is able to start recording by just pressing a button. When the *record* button is pressed, the application starts to play the video in another window, to record with the camera of the computer used in the experiment, and to record the streamed data of the *MUSE 2* headset. This allows the data to be easily synchronized for future steps, since the timestamps of the EEG and the recorded videos are the same as the video watched by the students, therefore there is no offset between the timestamps of the files.

By stopping the recording, the streamed EEG data is uploaded to a Google Drive folder in the form of comma-separated values (CSV). Each file contains five columns corresponding to the time and measurements obtained from the four electrodes. The name of the columns for the electrodes indicate which brain lobe they are associated with and contain their recorded data. The columns are titled as *AF7* (left frontal lobe), *AF8* (right frontal lobe), *TP9* (left temporal lobe) and *TP10* (right temporal lobe). The recorded video of the face of the participant is saved to an additional folder created in the computer where the experiment is taking place. The processing of both files is done separately and will be explained in the following sections.

B. Video processing

Four scripts were written to process the taken videos. All of them were developed using Python and the last one is a Jupyter Notebook.

The first script converts a 20 fps video to 10 fps, removing every other frame, therefore, the resulting video has the same duration as the original. This is achieved by using the *OpenCV* library. A function is applied to every video; this procedure goes through the frames with a counter that is increased by two in order to skip half of the frames and save half of them in the selected folder.

The second script divides the videos into smaller pieces according to an array that contains the limits in seconds of each section of the video. It calls a method that is applied to each video, it trims each part and saves it as an independent clip using the *FFMPEG* tools from the *MoviePy* library. All videos from the same section and different students are saved in the same folder, named after each section in short form: *I1* for irrelevant information part 1, *F1* for false information part 1, *R0* for relevant information, *F2* for false information part 2 and *I2* for irrelevant information part 2. The function contains a safety condition, since it prints a message in the console in case the recording is shorter than the video shown to the students, meaning that it does not contain all the sections.

The third script converts a video in images and saves the frames inside the selected folder. This uses an already trained face detector to save only the frames that contain a face for each video of each section. It also normalizes the size and color of the images by trimming the image to only save the faces of the participants in gray scale. The output images are the final data set for the next stage.

The last script is a Jupyter Notebook, it was done this way to easily observe the output for each part, since it involves heavier processing. This code was executed in Google Colab to benefit from their free use of GPU, which is why the images are compressed and extracted in the online environment. Since they are organized in folders representing their labels, the *image dataset from directory* function of the *Tensorflow* library is used to infer the pairs of image and label. The data set is split into training and validation set, the latter is formed by 25% of the images, as mentioned before.

Data augmentation is applied to better train the model, it is achieved by flipping and rotating a few degrees the original images, as well as decreasing their contrast. A backbone is created using the *EfficientNetB4*, already provided by *Tensorflow*, then two dense layers are created before the output layer. Cross entropy is used as the loss function. The model was executed for 180 epochs.

C. EEG data processing

For EEG analysis, several scripts in *MATLAB* were written and executed to process the raw signals.

The timestamps of the CSV files had to be normalized for accurate analysis; the first script was meant to do this by setting the step size according to the sample frequency of the headset (256 Hz). Labels were assigned to data according to important moments of the video, such as start and end of the video and the sections within it.

The video has 5 important moments that should be indicated in the data files, since they are the portions of data that will be analyzed. When the video starts, the students are given general instructions, then followed by irrelevant information, false information, relevant information, a second moment of false information, irrelevant information again and then it ends. The sections are brief but very well delimited in the video script design. A second script was created to filter and organize the raw signals. Executing this program allows to obtain them without noise and separated according to the already delimited frequency bands that are associated with different functional characteristics of activity in the brain. Five frequency bands (brainwaves) were obtained for each of the 4 electrode signals; theta (4-8 Hz), alpha (8-12 Hz), low beta (12-18 Hz), high beta (18-30 Hz) and gamma (30-100 Hz). The columns of these output files are composed of the timestamps, labels and all the combinations of the 5 frequency bands and the 4 electrodes. The third script computes the chaotic descriptors and builds a 4-dimensional point in the descriptor space for each section of the video in each column per student, because the frequency bands of each electrode were analyzed separately. The columns of the CSV output file are the student ID, electrode, frequency band, section (cluster), two parameters and the four chaotic descriptors: fractal dimension, Lyapunov exponent, Hurst exponent and approximate entropy.

Each group of points corresponding to a single section, a single electrode and a single frequency band needs to be tested against all the other groups to observe if there is a boundary that separates them in descriptor space. A fourth script was made to divide the CSV file in combinations of just two sections, one band and one electrode.

These files were separately loaded in *MATLAB*'s workspace as tables, then selected in the *Classification Learner* app. The response label and the one to be predicted by the trained models is the section, also called cluster. The predictors are the chaotic descriptors, which means they are the data that the selected models is going to be trained with in association with a label, also called class. The validation method of the classification is cross-validation; this involves dividing the data set into folds and each one of them gets to be the testing set, the rest is the training set, the accuracy of each fold is calculated and the mean accuracy is obtained. The cross-validation method protects against overfitting and the need for more data.

The models that were used and trained for this purpose in the *Classification Learner* app were all kinds of Decision Trees, Naive Bayes classifiers, Support Vector Machines (SVM) and Nearest Neighbor classifiers (KNN). The "History" window of the app shows all the executed models, the number of features or predictors used and the percentage of accuracy in the test.

III. Results

The ability that students had to use in this experiment was to distinguish relevant information from irrelevant and false information so they could perform the task indicated in the video. To see if this procedure has a clear difference of activity in the brain, the EEG signals of the sections were compared. Even if the type of information is the same, such as in *I1* and *I2* clusters, it is important to compare them too, since the brain could change its behavior from one to the other, Table II shows the classification performance between this sections.

Although it is important to mention that in a previous study, the false information sections were compared and the accuracy was not that good, which means the two sections of false information are not really differentiable. For this reason, from now on they will be handled as just one cluster, referred as *F*.

Next, the two irrelevant information sections were compared. Best results were obtained for the right temporal electrode and high beta frequency band, since 7 models obtained 100% accuracy, such as the three types of Trees, Naive Bayes and 2 types of SVM. This high accuracy was also obtained in the same electrode but in the low beta frequency band, as well as in the right frontal electrode, low beta and theta bands.

TABLE II
PERFORMANCE IN CLASSIFICATION OF SECTIONS I1 AND I2.

<table>
<tr><th>Electrode</th><th>Frequency band</th><th>Model type</th><th>Accuracy (%)</th></tr>
<tr><td rowspan="2">AF8</td><td>Low Beta</td><td>Gaussian NB
Cubic SVM</td><td rowspan="4">100</td></tr>
<tr><td>Theta</td><td>Medium Gaussian SVM
Linear SVM</td></tr>
<tr><td rowspan="2">TP10</td><td>High Beta</td><td rowspan="2">Fine Tree
Medium Tree
Coarse Tree
Gaussian NB
Kernel NB
Linear SVM
Quadratic SVM</td></tr>
<tr><td>Low Beta</td></tr>
</table>

When comparing false and relevant information (Table III), there was a clear boundary, since many combinations obtained 100% accuracy, such as the right temporal electrode with alpha, low beta and theta bands, and the left temporal electrode with high beta, alpha, theta and low beta bands.

The first section of irrelevant information was compared with all the false information data (Table IV). Complete accuracy was obtained with many combinations like the left frontal electrode with high beta and theta bands, right frontal electrode with high beta, low beta and theta bands, the right temporal electrode with high beta, low beta, theta and alpha bands, and left temporal electrode with low beta, theta and alpha bands.

About Table IV, it is important to mention that the frequency bands with superscripts have model types in common that also presented an accuracy value of 100%, which are presented in the last row of the corresponding electrode, with the superscripts representing the names of the corresponding frequency bands. Also, some rows in the model type column are shared with two rows of the frequency band column; this is made on purpose to simplify the table, and it means that both frequency bands presented an accuracy value of 100% in the model types written in the row that is shared between them.

The second section of irrelevant against false information (Table V) also showed 100% accuracy for the right temporal with the alpha frequency band, but only with SVM and KNN

TABLE III
PERFORMANCE IN CLASSIFICATION OF SECTIONS F AND R.

<table>
<tr><th>Electrode</th><th>Frequency band</th><th>Model type</th><th>Accuracy (%)</th></tr>
<tr><td rowspan="3">TP10</td><td>Alpha</td><td>Linear SVM
Quadratic SVM
Cubic SVM
Coarse Gaussian SVM
Medium KNN
Cosine KNN
Weighted KNN</td><td rowspan="7">100</td></tr>
<tr><td>Low Beta</td><td rowspan="2">Coarse Tree
Gaussian NB
Kernel NB
Linear SVM
Quadratic SVM
Cubic SVM
Medium Gaussian SVM
Coarse Gaussian SVM
Fine KNN
Medium KNN</td></tr>
<tr><td>Theta</td></tr>
<tr><td rowspan="4">TP9</td><td>High Beta</td><td>Fine Tree
Medium Tree
Coarse Tree</td></tr>
<tr><td>Alpha</td><td rowspan="2">Gaussian NB
Kernel NB
Linear SVM
Quadratic SVM
Cubic SVM
Medium Gaussian SVM
Coarse Gaussian SVM
Fine KNN
Medium KNN
Cubic KNN</td></tr>
<tr><td>Theta</td></tr>
<tr><td>Low Beta</td><td>Linear SVM
Medium Gaussian SVM
Coarse Gaussian SVM
Weighted KNN</td></tr>
</table>

models. The next best results for this comparison had a value of 97.9% in the same electrode but with the high beta and theta bands.

The first section of irrelevant information was now compared to the relevant information (Table VI), which did not gave complete accuracy, instead, the best result was obtained in the right temporal electrode with the high beta band and a value of 93.8% with just the Kernel Naive Bayes model. The second best results were obtained in the right frontal with the low beta frequency band and all the Tree models, the obtained accuracy was 90.6%.

The second section of irrelevant against relevant information (Table VII) had accuracy of 100% with both temporal electrodes with alpha, low beta and theta frequency bands. All of them with SVM models, as well as KNN models.

Results show distinct contrast between EEG and facial responses for relevant, irrelevant and false information.

First, for EEG data analysis, when comparing false and relevant information, there was a clear boundary, since many combinations of electrode and frequency obtained 100% accuracy, such as the both temporal electrodes with alpha, low beta and theta bands, shown in Fig. 1 It is worth to mention that plots shown here are 3-dimensional projections of the 4-dimensional descriptor space.

TABLE IV
PERFORMANCE IN CLASSIFICATION OF SECTIONS I1 AND F.

Electrode	Frequency band	Model type	**Accuracy** (%)
AF7	High Beta	Weighted KNN	**100**
	Theta	Gaussian NB Kernel NB	
AF8	High Beta[1]	Fine Tree Medium Tree	
		Gaussian NB Kernel NB	
	Low Beta[2]	Coarse Gaussian SVM Fine KNN	
	Theta[3]	Coarse Gaussian SVM Fine KNN Medium KNN	
	1 2 3	Coarse Tree Linear SVM Quadratic SVM Cubic SVM Medium Gaussian SVM	
TP10	High Beta[4]	Coarse Tree Kernel NB Cubic SVM	
	Low Beta[5]	Medium KNN	
	Alpha[6]	Coarse Tree Cubic SVM	
	Theta[7]	Medium SVM Cosine KNN Cubic KNN	
	4 5 6 7	Gaussian NB Linear SVM Quadratic SVM Medium Gaussian SVM Coarse Gaussian SVM Fine KNN	
TP9	Low Beta	Fine Tree Medium Tree Coarse Tree	
	Theta[8]	Medium Gaussian SVM Fine KNN	
	Alpha[9]	Kernel NB Linear SVM Coarse Gaussian SVM	
	8 9	Quadratic SVM Cubic SVM Medium KNN Cubic KNN Weighted KNN	

TABLE V
PERFORMANCE IN CLASSIFICATION OF SECTIONS I2 AND F.

Electrode	Frequency band	Model type	**Accuracy** (%)
TP10	Alpha	Linear SVM Medium Gaussian SVM Medium KNN Cubic KNN Weighted KNN	**100**
	High Beta	Linear SVM Medium Gaussian SVM Medium KNN Cosine KNN Cubic KNN Weighted SVM	**97.9**
	Theta	Gaussian NB Linear SVM Quadratic SVM Cubic SVM Medium Gaussian SVM Fine KNN	

TABLE VI
PERFORMANCE IN CLASSIFICATION OF SECTIONS I1 AND R.

Electrode	Frequency band	Model type	**Accuracy** (%)
TP10	High Beta	Kernel NB	**93.8**
	Low Beta	Fine Tree Medium Tree Coarse Tree	**90.6**

TABLE VII
PERFORMANCE IN CLASSIFICATION OF SECTIONS I2 AND R.

Electrode	Frequency band	Model type	**Accuracy** (%)
TP10	Alpha	Linear SVM	**100**
	Low Beta	Gaussian NB Kernel NB	
	Theta	Kernel NB Linear SVM Quadratic SVM Cubic SVM Medium Gaussian SVM Coarse Gaussian SVM Fine KNN Medium KNN Cosine KNN Cubic KNN Weighted KNN	
TP9	Alpha	Linear SVM	
	Low Beta	Linear SVM Quadratic SVM	
	Theta	Quadratic SVM	

The first section of irrelevant information was compared with all the false information data. Complete accuracy was also obtained with many combinations like both frontal electrodes with high beta and theta bands, as well as both temporal electrodes with low beta, theta and alpha bands.

The first section of irrelevant information was now compared to the relevant information, which did not gave complete accuracy, instead, the best result was obtained in the right temporal electrode with the high beta band and a value of 93.8% with just the Kernel Naive Bayes model. The second best results were obtained in the right frontal with the low beta frequency band and all the Tree models, the obtained accuracy was 90.6%. However, the second section of irrelevant against relevant information had accuracy of 100% with both temporal

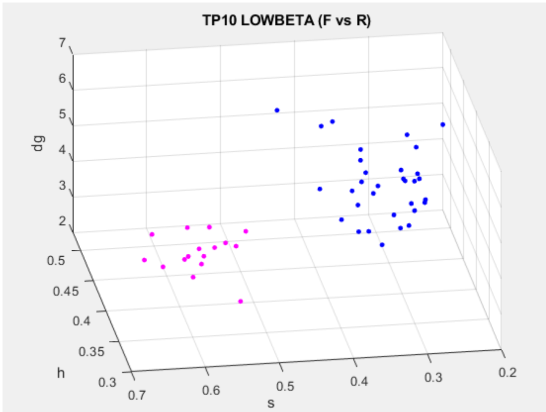

Fig. 1. Points in 3-dimensional projection of the descriptor space for false information (F, blue points) and relevant information (R, magenta points) measurements of the right temporal electrode (TP10) in the low beta frequency band.

electrodes with alpha, low beta and theta frequency bands, shown in Fig. 2. All of them with SVM models, as well as KNN models.

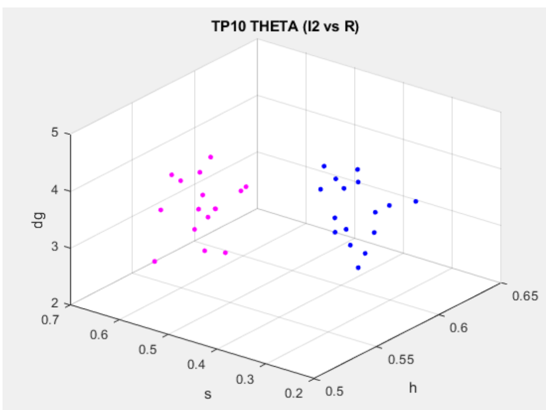

Fig. 2. Points in 3-dimensional projection of descriptor space for irrelevant information 2 (I2, blue points) and relevant information (R, magenta points) measurements of the right temporal electrode (TP10) in the theta frequency band.

A. Video analysis

The accuracy obtained with the `EfficientNetB4` was 95.69% with 180 epochs. It can be observed in Fig. 3 that the values are beginning to converge. The number of epochs was chosen according to the technology capacities of the computer where the analysis of the data took place and the limitations of the environment provided in Google Colab. No image samples are shown here to preserve personal data of students.

IV. Conclusions

With the gathered results of the various classification models and the plots of data points in descriptor space, the first result that stands out is the great difference between the false information with all the other clusters, including both irrelevant and relevant information moments. The electrodes

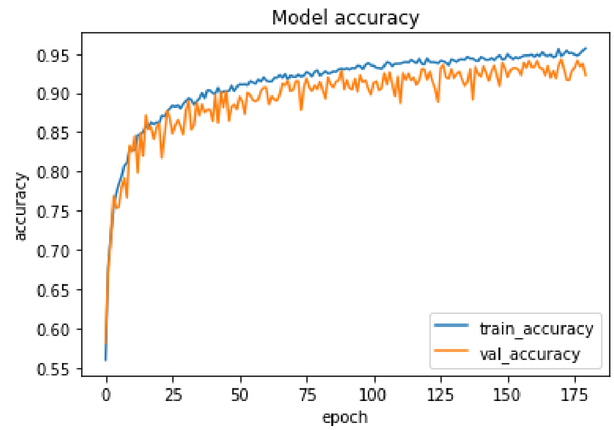

Fig. 3. Computed train and validation accuracy through the number of epochs.

that were closely associated with the differentiation of false information were those corresponding to both temporal lobes and the frequency bands with more relevance were alpha, beta and theta. This could be because it is quicker to point out a fact is false, specially when the contra-argument has been learned before. On the other hand, for facial recognition, good results were obtained corresponding to those obtained with EEG analysis.

Acknowledgment

The authors would like to acknowledge the financial support of Writing Lab, Institute for the Future of Education, Tecnologico de Monterrey, Mexico, in the production of this work. The authors would like to acknowledge the financial support of Novus Grant with PEP No. PHHT085-21ZZNV049, TecLabs, Tecnologico de Monterrey, Mexico, in the production of this work.

References

[1] S. Scepanovič, "The fourth industrial revolution and education," in *2019 8th Mediterranean Conference on Embedded Computing (MECO)*, pp. 1–4, IEEE, 2019.

[2] H. G. González-Hernández, J. M. Medina-Pozos, V. Cantú-González, A. Amozurrutia-Elizalde, A. Flores-Amado, and R. J. Mora-Salinas, "Looking for experimental evidence of critical thinking through eeg," *International Journal on Interactive Design and Manufacturing (IJIDeM)*, vol. 15, no. 2, pp. 333–351, 2021.

[3] V. Kalyan Kumar, P. Suja, and S. Tripathi, "Emotion recognition from facial expressions for 4d videos using geometric approach," in *Advances in Signal Processing and Intelligent Recognition Systems: Proceedings of Second International Symposium on Signal Processing and Intelligent Recognition Systems (SIRS-2015) December 16-19, 2015, Trivandrum, India*, pp. 3–14, Springer, 2016.

[4] G. Patil and P. Suja, "Emotion recognition from 3d videos using optical flow method," in *2017 International Conference On Smart Technologies For Smart Nation (SmartTechCon)*, pp. 825–829, IEEE, 2017.

[5] N. Hajarolasvadi, E. Bashirov, and H. Demirel, "Video-based person-dependent and person-independent facial emotion recognition," *Signal, Image and Video Processing*, vol. 15, pp. 1049–1056, 2021.

[6] N. Samadiani, G. Huang, Y. Hu, and X. Li, "Happy emotion recognition from unconstrained videos using 3d hybrid deep features," *IEEE access*, vol. 9, pp. 35524–35538, 2021.

[7] K. S. Rao and S. G. Koolagudi, "Recognition of emotions from video using acoustic and facial features," *Signal, Image and Video Processing*, vol. 9, pp. 1029–1045, 2015.

[8] G. Kavalakis, N. Vidakis, and G. Triantafyllidis, "Emotion index of cover song music video clips based on facial expression recognition," in *Interactivity, Game Creation, Design, Learning, and Innovation: 5th International Conference, ArtsIT 2016, and First International Conference, DLI 2016, Esbjerg, Denmark, May 2–3, 2016, Proceedings 5*, pp. 248–255, Springer, 2017.

[9] M. Hu, Q. Chu, X. Wang, L. He, and F. Ren, "A two-stage spatiotemporal attention convolution network for continuous dimensional emotion recognition from facial video," *IEEE Signal Processing Letters*, vol. 28, pp. 698–702, 2021.

[10] H. Qayyum, M. Majid, S. M. Anwar, and B. Khan, "Facial expression recognition using stationary wavelet transform features," *Mathematical Problems in Engineering*, vol. 2017, 2017.

[11] P. Tamil Selvi, P. Vyshnavi, R. Jagadish, S. Srikumar, and S. Veni, "Emotion recognition from videos using facial expressions," in *Artificial Intelligence and Evolutionary Computations in Engineering Systems: Proceedings of ICAIECES 2016*, pp. 565–576, Springer, 2017.

[12] T. Kalsum, S. M. Anwar, M. Majid, B. Khan, and S. M. Ali, "Emotion recognition from facial expressions using hybrid feature descriptors," *IET Image Processing*, vol. 12, no. 6, pp. 1004–1012, 2018.

[13] H. Salih and L. Kulkarni, "Study of video based facial expression and emotions recognition methods," in *2017 international conference on I-SMAC (IoT in social, mobile, analytics and cloud)(I-SMAC)*, pp. 692–696, IEEE, 2017.

[14] A. R. Pathak, S. Bhalsing, S. Desai, M. Gandhi, and P. Patwardhan, "Deep learning model for facial emotion recognition," in *Proceedings of ICETIT 2019: Emerging Trends in Information Technology*, pp. 543–558, Springer, 2020.

[15] S. Saganowski, "Bringing emotion recognition out of the lab into real life: Recent advances in sensors and machine learning," *Electronics*, vol. 11, no. 3, p. 496, 2022.

[16] S. Wu, Z. Du, W. Li, D. Huang, and Y. Wang, "Continuous emotion recognition in videos by fusing facial expression, head pose and eye gaze," in *2019 International Conference on Multimodal Interaction*, pp. 40–48, 2019.

[17] S. Wang, Z. Liu, Y. Zhu, M. He, X. Chen, and Q. Ji, "Implicit video emotion tagging from audiences' facial expression," *Multimedia Tools and Applications*, vol. 74, pp. 4679–4706, 2015.

[18] N. Hajarolasvadi and H. Demirel, "Deep facial emotion recognition in video using eigenframes," *IET Image Processing*, vol. 14, no. 14, pp. 3536–3546, 2020.

[19] D. Y. Choi, D.-H. Kim, and B. C. Song, "Multimodal attention network for continuous-time emotion recognition using video and eeg signals," *IEEE Access*, vol. 8, pp. 203814–203826, 2020.

[20] Y. Yang, Q. Gao, X. Song, Y. Song, Z. Mao, and J. Liu, "Facial expression and eeg fusion for investigating continuous emotions of deaf subjects," *IEEE Sensors Journal*, vol. 21, no. 15, pp. 16894–16903, 2021.

[21] D. Li, Z. Wang, C. Wang, S. Liu, W. Chi, E. Dong, X. Song, Q. Gao, and Y. Song, "The fusion of electroencephalography and facial expression for continuous emotion recognition," *IEEE Access*, vol. 7, pp. 155724–155736, 2019.

[22] M. Soleymani, S. Asghari-Esfeden, Y. Fu, and M. Pantic, "Analysis of eeg signals and facial expressions for continuous emotion detection," *IEEE Transactions on Affective Computing*, vol. 7, no. 1, pp. 17–28, 2015.

[23] G. Du, S. Long, and H. Yuan, "Non-contact emotion recognition combining heart rate and facial expression for interactive gaming environments," *IEEE Access*, vol. 8, pp. 11896–11906, 2020.

[24] M. Sharafi, M. Yazdchi, R. Rasti, and F. Nasimi, "A novel spatio-temporal convolutional neural framework for multimodal emotion recognition," *Biomedical Signal Processing and Control*, vol. 78, p. 103970, 2022.

[25] S. Saganowski, J. Komoszyńska, M. Behnke, B. Perz, D. Kunc, B. Klich, Ł. D. Kaczmarek, and P. Kazienko, "Emognition dataset: emotion recognition with self-reports, facial expressions, and physiology using wearables," *Scientific data*, vol. 9, no. 1, p. 158, 2022.

[26] H. G. Gonzalez-Hernandez, D. V. Peña-Cortes, A. Flores-Amado, A. Amozurrutia-Elizalde, and R. J. Mora-Salinas, "Decreasing exam-anxiety levels with mindfulness through eeg measurements," in *2022 IEEE Global Engineering Education Conference (EDUCON)*, pp. 1213–1220, IEEE, 2022.